Check for updates

On the relationship of morphology evolution and thermal conductivity of flax reinforced polypropylene laminates

Masoud Bodaghi[1]*, Doriane Delfrari[1], Margot Lucas[1], Noha-Lys Senoussaoui[1], Yao Koutsawa[1], Burcu Karaca Uğural[2] and Henri Perrin[1]

[1]Luxembourg Institute of Science and Technology (LIST), Hautcharage, Luxembourg, [2]Head Office, BPREG, Bornova, Izmir, Türkiye

This paper focuses on the morphology evolution in the forming process of unidirectional flax reinforced polypropylene composite laminates. The link between the morphology evolution and thermal conductivity during consolidation stages is investigated. Hot press forming allows to manufacture several composite laminates at different consolidation stages as a function of the compaction thickness. Microscopic evolution of the laminates in terms of morphology and porosity fractions are evaluated by scanning electron microscopy and X-ray microtomography (μ-CT). Hot disk technique is applied to measure the thermal conductivity of the laminates in in-plane and transverse directions. It is found that the in-plane thermal conductivity almost linearly increases with the reduction of porosity fraction. However, the transverse thermal conductivity remained constant. Beside the proposed relations, a theoretical model, based on a two-level Mori-Tanaka homogenization method is proposed. Considering the three-phases material (i.e., porosity, fiber, and polymer matrix), there is a good agreement between the experiment data and model predictions, but limited predictivity for porosity level above 15% certainly due to simplifying assumptions used in the predictive model.

KEYWORDS

thermal conductivity, flax fiber, hot press forming, consolidation, porosity

1 Introduction

Given the increasing demand for fiber reinforced polymer composites from aerospace to marine and infrastructure industry sectors, the global solidarity solution is sustainable composite products with the lowest ecological footprint during and at the end of their service life has been a major industry driver of polymer composite materials. Natural fiber reinforced composites can potentially reduce the global dependence on the petroleum-based fibers such as glass and carbon. In addition, a shift from thermoset composites to the thermoplastic counterparts accelerates manufacturing cycle, improves toughness and impact strength, and allows a reliable recycling process. Therefore, natural fiber reinforced thermoplastic composites will be a material platform for circular economy.

TABLE 1 Experimental study of thermal conductivity measurements of different types of natural fiber reinforced thermoplastic or thermoset composites.

References	Composite		Fabric structure	V_f (%) range	Manufacturing technique	Thermal conductivity (W/mK) range		Test method
	Fiber	Resin				In-plane	Transverse	
Mishra et al. (2020)	Flax	Epoxy	plain weave	35–37	Hand lay-up and hot press molding	----	0.27–0.31	C-therm TCi
	Jute		twill weave					
			Unidirectional				0.25–0.26	
			Matt					
Wang et al. (2020)	Bamboo	polypropylene fiber	Non-woven	36–74	hot press molding		0.03–0.35	HotDisk transient plane source (TPS) −2500s
Zheng (2014)	Hemp	----	Unidirectional	100	------	----	0.12	Numerical modelling
Mounika et al. (2012)	Bamboo	Polyester	Unidirectional	15–60	Hand lay-up and hot press molding		0.18–0.21	Guarded heat floy meter
Thilagavathi et al. (2010)	mix (bamboo, banana, and jute fibers)	polypropylene fiber	Non-woven	49.4	Web formation and subsequent needle-punching machine	-----	0.03	ASTM D 737
Li et al. (2008)	flax (NaOH treatment)	high density polyethylene	Powder	6.8–21.9	Extrusion	-----	0.32–0.42	Line-source
Behzad and Sain (2007)	Hemp	Acrylic polymer	Random	50–80	Vacuum infusion	0.74–0.97	0.18–0.28	Davidson&James
Takagi et al. (2007)	Bamboo	Poly lactic acid (PLA)	Chopped random	61.8	hot press molding	------	0.34	Hot wire
Kim et al. (2006)	mix (kenaf/ hemp/flax/ sisal)	maleated polypropylene	Chopped random	38–42	hot press molding	-----	0.05–0.06	ASTM-C518 (steady state)
Mangal et al. (2003)	Pineapple leaf	phenol formaldehyde and coupling agent	Unidirectional	------	Fiber treatment	--------	0.12–0.22	HotDisk TPS

The standard materials for continuous natural fiber reinforced thermoplastic composites are prepreg or semipreg (comingled yarn-based fabric). These semi-products open the way to new forming techniques such as hot press forming (Ouagne et al., 2010; Bourmaud et al., 2016; Derbali et al., 2018), automated prepreg tape placement (Lukaszewicz et al., 2012; van Hoa et al., 2017; Donough et al., 2022), or new welding techniques (Ageorges et al., 2001; Ageorges and Ye, 2002; Yousefpour et al., 2004; Fu et al., 2022). One of the very influent parameters of the forming techniques is the temperature (Guzman-Maldonado et al., 2016). The careful design of temperature cycle can maximize the process window and minimize the porosity volume fraction of fabricated composites (Hernández et al., 2013). Improper process design could lead to a porosity volume fraction of 30% (Madsen et al., 2007). Porosity formation during thermoplastic prepreg consolidation is referred to the empty spaces between the stacked prepreg layers (inter-layer porosities) and within the layers (intra-layer porosities).

Certain increase in the processing temperature of stacked prepreg layers decreases the resin viscosity, enhances the impregnation property of a thermoplastic resin to a reinforcing fiber, and hence evolves contact layers (Saenz-Castillo et al., 2019). But temperature must be kept below a maximum value to avoid the thermal degradation of natural fiber reinforcing thermoplastic composites (Gassan and Bledzki, 2001; van de Velde and Baetens, 2001; Fujihara et al., 2004). A well-consolidated natural fiber reinforcing thermoplastic composites must be conducted within a narrow window of opportunity. Recognizing the thermal properties such as thermal conductivity at processing temperatures are important parameters to simulate the temperature gradient inside the composite during a forming process (Li et al., 2008). Barasinski et al. (Barasinski et al., 2011) observed non-continuous temperature field between layers during thermoplastic tape placement process due to the existence of inter-layer porosities. They remarked that the evolution of the layer contacts improves the thermal conductivity across the material. The thermal conductivity of fiber and polymer within a prepreg makes an important contribution to the heat transfer. On the other hand, porosities across the composite volume can significantly influence the thermal behavior of a stacked prepreg during a thermoforming process.
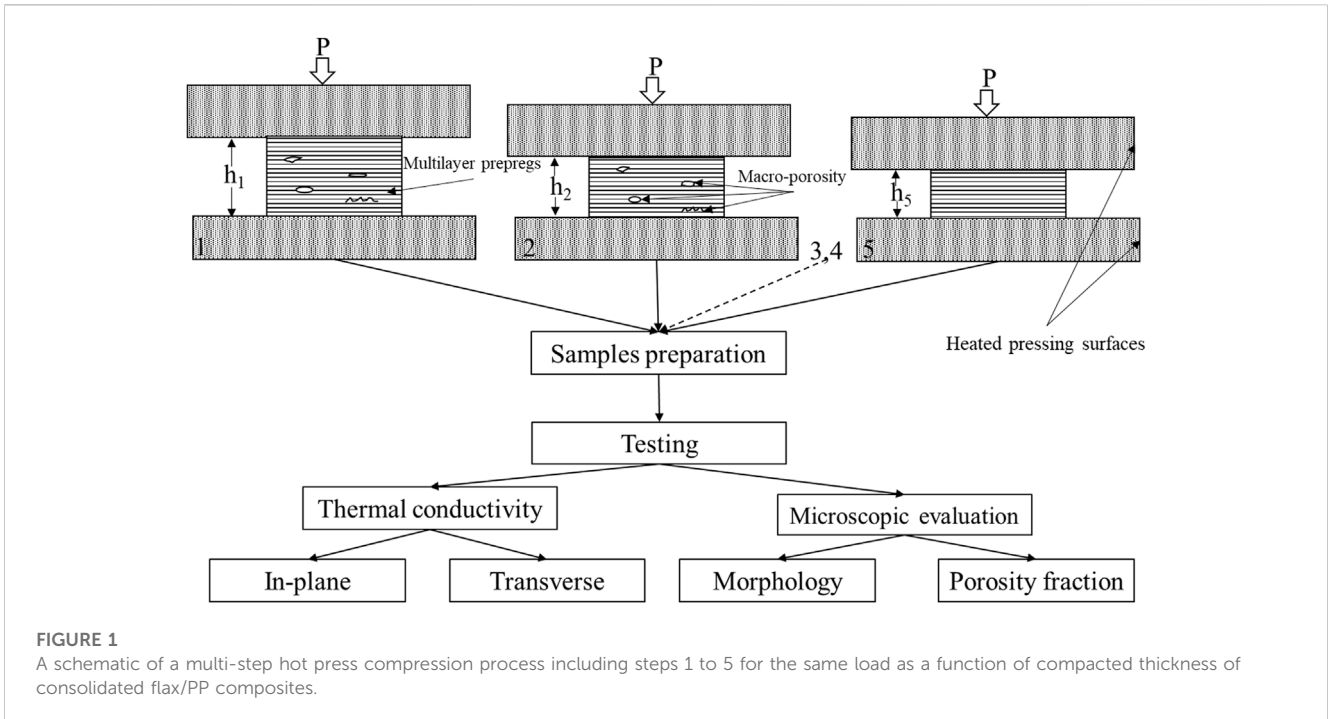
FIGURE 1
A schematic of a multi-step hot press compression process including steps 1 to 5 for the same load as a function of compacted thickness of consolidated flax/PP composites.
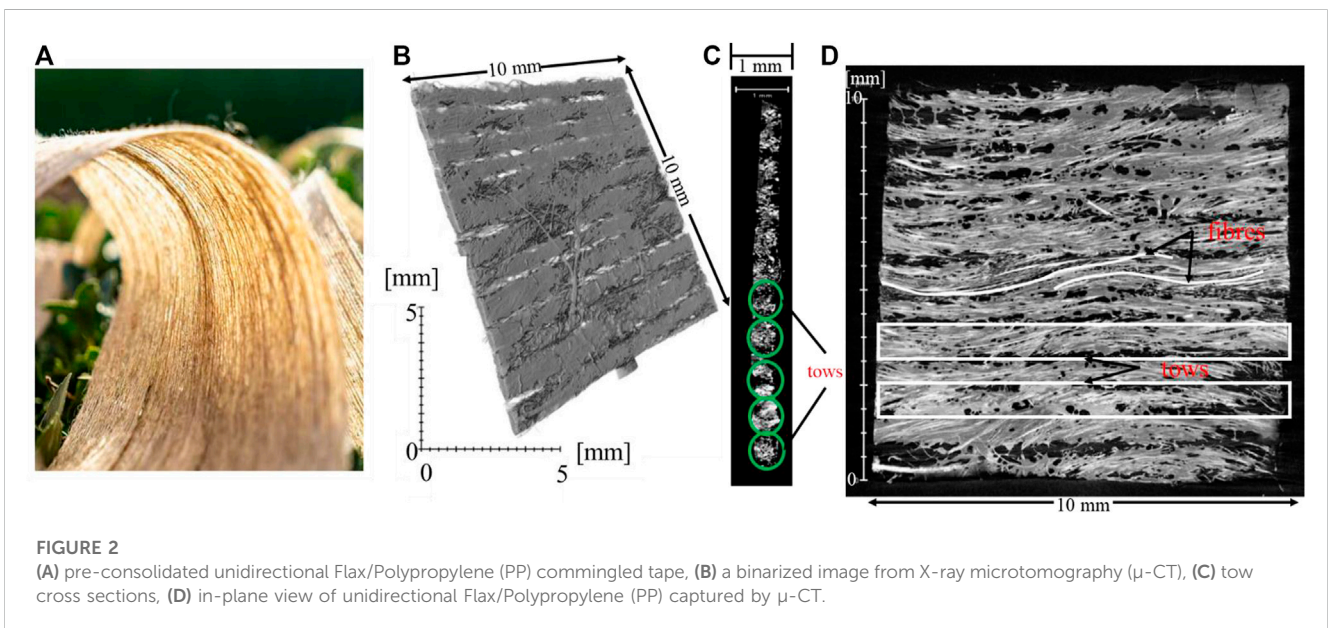

FIGURE 2
(A) pre-consolidated unidirectional Flax/Polypropylene (PP) commingled tape, **(B)** a binarized image from X-ray microtomography (μ-CT), **(C)** tow cross sections, **(D)** in-plane view of unidirectional Flax/Polypropylene (PP) captured by μ-CT.

TABLE 2 The technical specifications of the Flax/Polypropylene (PP) commingled unidirectional fabric (BPREG, 2022).

Supplier	Fibre content (wt%)	Polymer type	Consolidated ply thickness (mm)	Width (cm)	Areal density (g/m²)
BPREG	50	semi-crystalline Polypropylene (PP)	0.3	60	300

Given the lower value of the thermal conductivity of air compared with a solid, the incorporation of porosity into a stacked prepreg decreases its thermal conductivity.

Non-etheless, no author addressed the link between the porosity fraction and thermal conductivity, especially when the morphology of a composite laminate is evolving during a consolidation or forming process.

FIGURE 3
Schematic diagram of the confined compression hot-press forming.
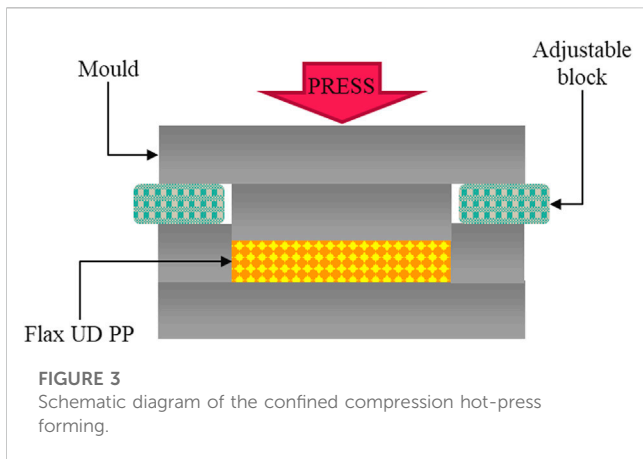
1.1 Previous work and objectives

Although much research has been carried out on natural fiber composites, little is known about the relationship of thermal conductivity and the microstructure evolution of natural fiber reinforced thermoplastic composite during forming process. Exiting studies majorly focused on the relationship of transverse thermal conductivity and fiber content for the fully consolidated natural fiber reinforced polymer composites (see Table 1).

Thermal conductivity of stacked prepreg layers is not a simple function of the thermal conductivities of its components, (i.e., polymer, and fiber) during a consolidation step. It is strongly affected by porosity fraction, pore geometries and microstructural evolution. The relation between fibres microstructure and its evolution during processing has been documented in the literature (Dumont et al., 2010; Latil et al., 2011; Dumont et al., 2017). The effect of microstructure characteristics such as fibre diameter and orientation angle on the conductivity of fibrous media has been also discussed (Fu and Mai, 2003; Han and Chung, 2011; Lu et al., 2021). However, the effect of microstructure on the thermal conductivity, accounting for the third phase (porosity), has yet to be evaluated. Thermoplastic prepreg materials contain a relatively high level of initial porosity content (intra-layer porosity) (5%–10%) (Zhang et al., 2017). Because of the rough prepreg surface, large inter-layer porosities are expected for multi-layered prepreg. Intra-layer porosities are as important a limiting factor as inter-layer porosities in thermal conductivity. During the consolidation, after the thermoplastic composites is heated, a compression pressure is applied to reduce intra- and inter-layer porosities. A few papers have reported the correlation between microstructure evolutions as a function of inter-layer porosity fraction and thermal conductivity during a consolidation process. Most of these studies simplified the geometry of inter-layer porosities rather than a complete porosity measurement. Lee and Springer (il Lee and Springer, 1987) modelled the degree of layer contact evolution as a function of temperature and pressure by using a succession of rectangular asperities. Although Yang and Pitchumani (Yang and Pitchumani, 2001) improved the geometrical description of layer contact evolution, the literature (Mantell and Springer, 1992; Ageorges et al., 2001; Lamèthe et al., 2005; Tierney and Gillespie, 2006; Khan et al., 2010) widely applied the model of (il Lee and Springer, 1987). Levy et al. (Lévy et al., 2014) made use of Lee and Springer's model (il Lee and Springer, 1987) to relate

layer contact evolution between layers of a laminate and internal thermal contact resistance under constant pressure and isothermal conditions. However, those works were developed for a thin layer which is composed of two phases: a composite phase and an air phase. They also ignored the incorporation of the intra-layer porosities into their model. The reduction of intralayer porosities is dominated by the porosity consolidation under the effect of a compaction pressure. After the compression of a stacked prepreg, the thickness is changing, and the resin flows to fill the porosities. Depending on the spatial distribution and local content of intra-layer porosity within prepregs, some intra-layer porosities are difficult to be removed (Zhang et al., 2017), (Simacek et al., 2013). To our best knowledge, the sole study in the view of microstructure of plant fiber and composite has been provided by Liu et al. (Liu et al., 2014). They showed that the transverse thermal conductivity of unidirectional abaca fiber/epoxy composite manufactured by resin transfer molding (RTM) increases by decreasing porosity fraction and increasing weakest linkage strength. Porosities in thermosetting composites can be washed out with resin flow, bleeding introduced high pressure, vibration, and vacuum in RTM process (Mehdikhani et al., 2019). Intralayer and interlayer porosities in thermoplastic composites is hard to be eliminated due to the high viscosity of thermoplastic resins (10^5–10^9 mPa s for thermoplastic melt vs. 30–200 mPa s) that results in significantly limited resin flow comparing to thermosetting counterparts such as epoxy (van Rijswijk and Bersee, 2007).

The objective of the present work is to determine thermal conductivity in in-plane and transverse directions at different porosity fractions as a function of compacted thickness of consolidated composites. During the consolidation step (Figure 1), the load (p) is applied on the flax fibre thermoplastic prepreg above the melting temperature of semi-crystalline polypropylene (PP). This load forces the molten thermoplastic to be impregnated into the flax fabrics while gradually removing porosities. Change at the thicknesses ($h_1 > h_2 > \ldots > h_5$) will be the controlling parameter for the morphology evolution and obtained porosity fraction. Thermal conductivities are measured at five different consolidation stages by using a Hot disk technique. Finally, a correlation with theoretical values, based on measured and estimated inputs parameters is proposed. Figure 1 represents the steps involved in the evolution of composite microstructure at different consolidation stages for the same load (p).

2 Experiments

2.1 Materials

The tested material is a pre-consolidated unidirectional Flax/semi-crystalline Polypropylene (PP) commingled tape (Figure 2A) supplied by BPREG. The main properties of the fabric are summarized in Table 2.

With X-ray microtomography (μ-CT), Figure 2B shows white rodlike porosities in a pre-consolidated unidirectional Flax/Polypropylene (PP) commingled tape. The cross-sectional images of fibre tows are shown in Figure 2C. The width of ellipse-shaped tow cross sections (green in Figure 2C) is around 600 μm. The in-plane view of a tow captured by μ-CT has a deviation from a straight
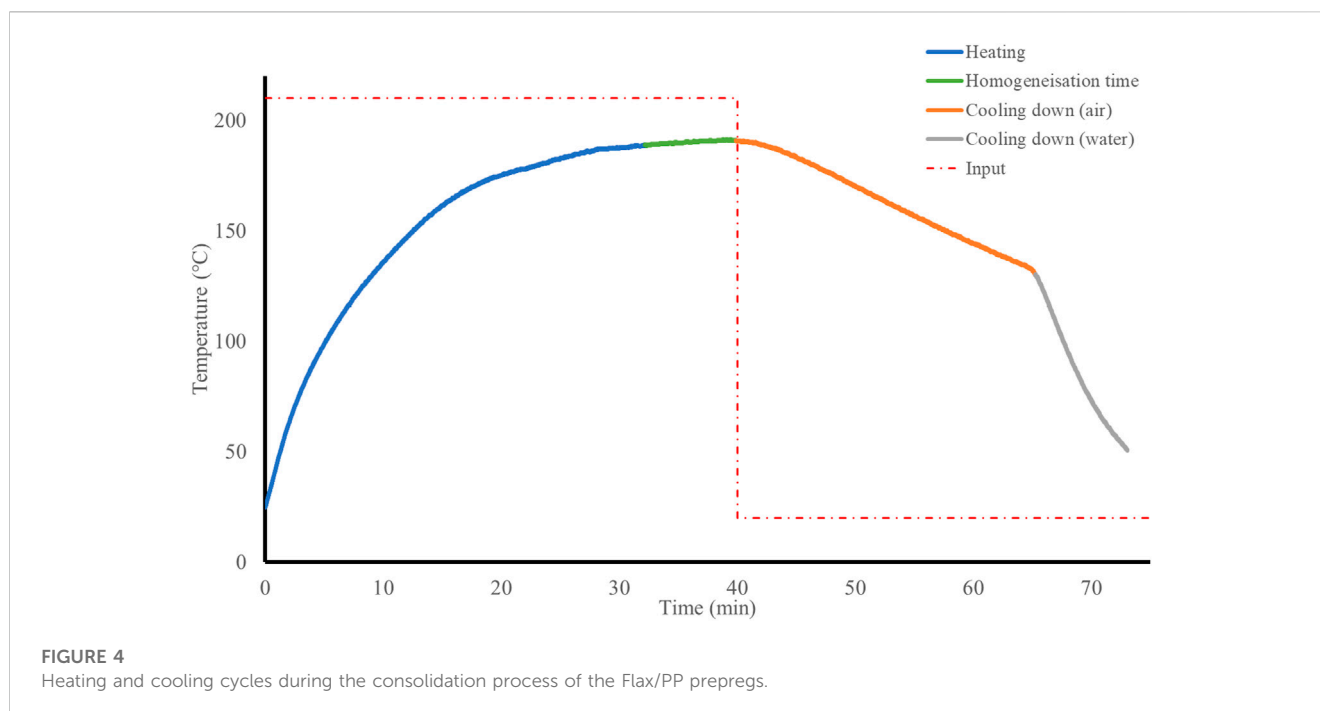
FIGURE 4
Heating and cooling cycles during the consolidation process of the Flax/PP prepregs.

TABLE 3 Series of experiments for morphology evolution and thermal conductivity measurements. The thickness percentage reduction was calculated relative to the primary consolidation stage.

Thickness percentage reduction	0%	7%	12%	20%	25%
Consolidation stages	1 (primary consolidation)	2	3	4	5 (fully consolidated)
Spacer blocks for the first series of experiments (mm)	5.80	5.40	5.0	4.60	4.30
Spacer blocks for the second series of experiments (mm)	16.60	15.50	14.60	13.10	12.50

line as shown in Figure 2D. This inherent deviation, which is not visible by naked eye, is due to the tow twisting during the manufacturing process of a pre-consolidated unidirectional Flax/PP commingled tape.

2.2 Fabrication of neat PP and its composite laminates

The thermal conductivity of a polymer composite is influenced by several factors including, fiber direction, fiber volume fraction, moisture content, porosity fraction and polymer type. The major contributors to the thermal conductivity changes are fiber and porosity fractions and the conductive characteristics of polymer and fiber. In this study, in addition to the composite samples, one sample of neat PP was also manufactured by a hot-press forming process.

2.2.1 Neat PP manufacturing

To minimize the thermal degradation during hot-press forming, the thermal behavior of PP polymer was characterized by differential scanning calorimetry (DSC) and thermal gravimetric analysis (TGA). The test specimen was dried at 80°C for 1 hour. DSC results showed melting temperature of 165°C for PP. The isothermal TGA results at 190°C for 2 h determined 2 wt% degradation of PP. Accordingly, the neat PP plates were fabricated by hot press forming at 190°C as follows: polypropylene fibers were placed inside a preheated square mold having dimensions of 100 × 100 mm^2. The plate thickness was adjusted by using picture frame of 15 mm. Subsequently, the mold was closed with a pressure of 10 bars for 10 min. The plate was demolded at temperatures below 30°C. Finally, the samples were cut from the plates for thermal conductivity measurements.

2.2.2 Consolidation of unidirectional Flax/PP composite

To avoid the thermal degradation, after oven drying at 80°C for one night, isothermal TGA of dried flax fibre at 190°C was also performed for 2 h. The TGA results showed a negligible degradation (>1%) of flax fibres. The consolidation process is like the one applied for the fabrication of neat PP. In this work, only the influence of the mold cavity nominal thickness on the porosity fraction, morphology evolution and thermal conductivity is considered. At each consolidation iteration, the subsequent change in cavity height is applied to the thickness of the consolidated flax/PP composite. The reference sample was defined from the minimum achievable
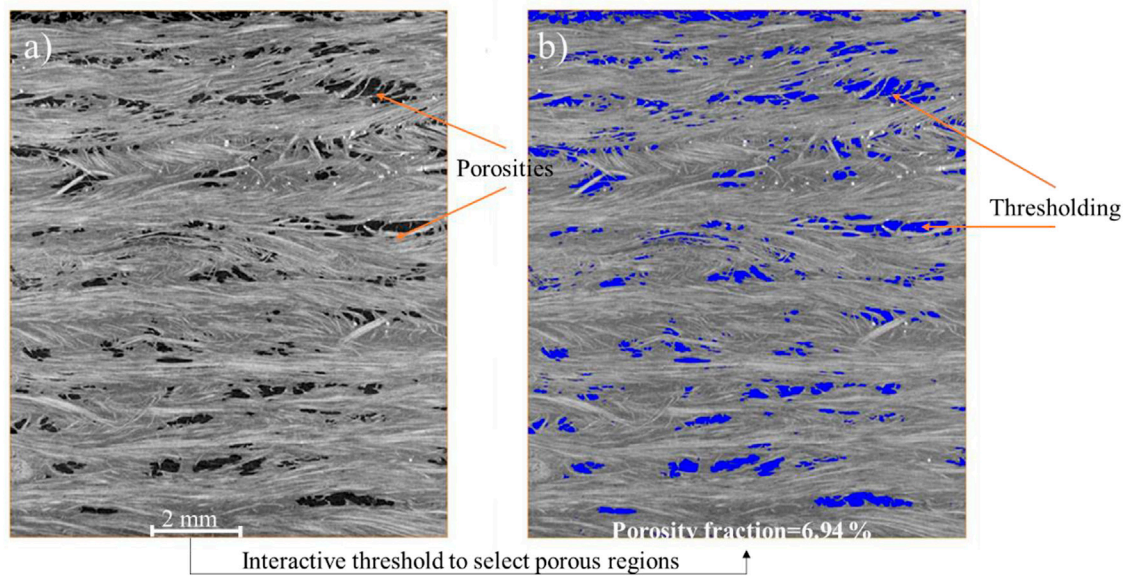
FIGURE 5
(A) A grayscale tomographic slice of the flax/PP specimen with 7% thickness reduction relative to the base line (i.e., consolidation stage 2), **(B)** the image of tomographic slice of the flax/pp specimen processed by Avizo software, highlighting porous regions in blue.
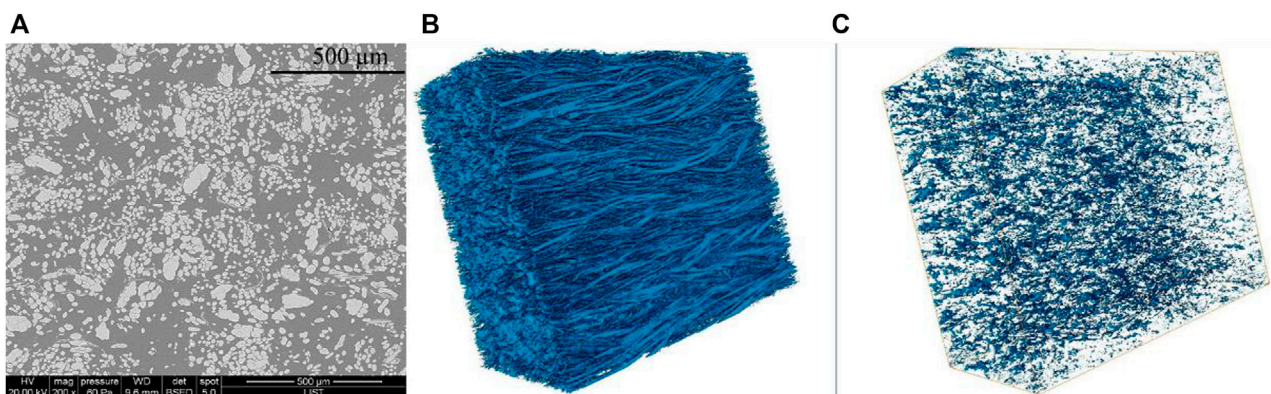

FIGURE 6
Fully consolidated ten-layer flax/pp composite: **(A)** cross-sectional morphology of consolidated image, **(B)** 3D image of fibers from micro-CT, **(C)** 3D image of porosities from micro-CT with the following operating conditions: voltage: 70 kV; current: 160 μA, isotropic voxel size: 6 × 6 × 6 μm, scan time: 90 min.

thickness at which the porosities are almost eliminated, and fiber volume fraction reaches to its maximum. In this study, our reference sample was achieved at the cavity height of 2.3 mm. Based on the obtained reference thickness, four intermediate consolidation states were conducted by changing mold cavity with the same pressure load. The percentages of thickness reduction were 0%, 7%, 12%, 20%, 25% relative to the thickness of the primary consolidation. The mould tooling and Flax/PP assembly inside the cavity is shown in Figure 3. The upper and bottom compaction surfaces were steel plates. Consolidation process as follows: the composite from a dried stack of Flax/PP prepreg layers (after oven drying at 80°C for one night) was molded and subsequently closed with a gap of 50 μm to

outflow the excess molten polymer during compression stage. The mold was put on a hot-press machine preheated to 200°C. As soon as the mold reached to the temperature of 190°C, it was held for 10 min without compression to allow the PP to start melting and percolating through the fibers. Subsequently, the assembly was pressed at 1 mm/ min constant closing speed to reach the target thickness and held for 10 min for consolidation. The target thickness was adjusted by standard spacer blocks (see Figure 3).

During the consolidation, the applied pressure (10 bar) forced the molten polymer to fill the empty spaces between and inside the fibre tows while eliminating porosities. During the cooling period, the pressure applied was maintained until the temperature of the
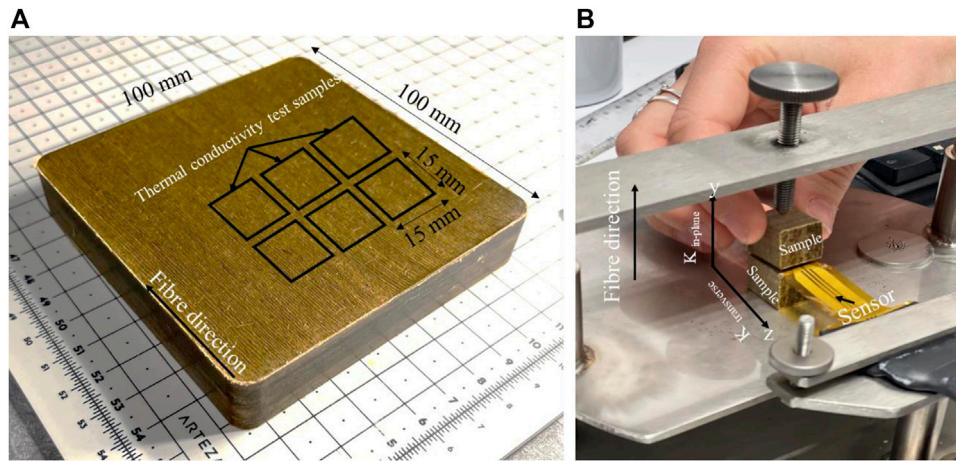
FIGURE 7
Schematic illustration of thermal conductivity measurement by using Hot Disk technique. **(A)** sample preparation, **(B)** TPS assembly.
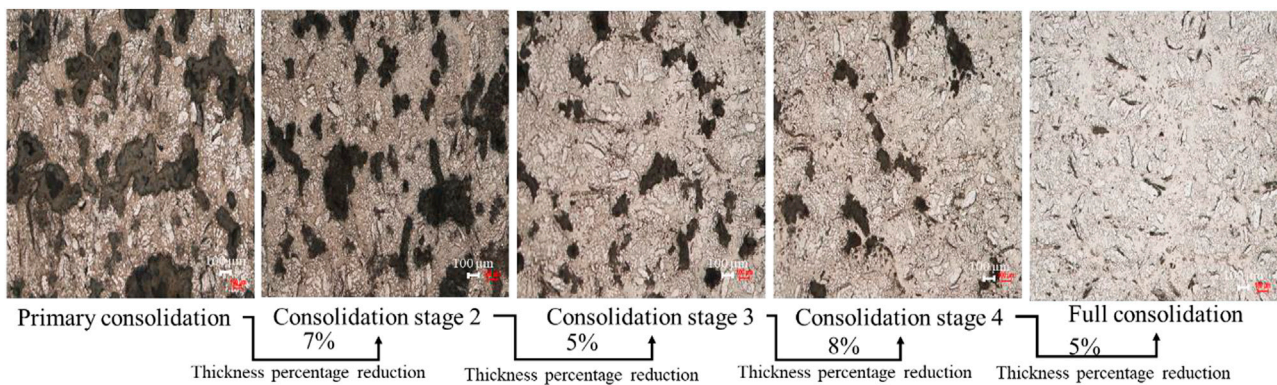

FIGURE 8
SEM observations for microstructure changing of flax/pp composites under consolidation stages: morphology changes as a function of the thickness percentage reduction at different consolidation stages.

mold cavity dropped down to 50°C for demolding the consolidated laminate. Improper cooling cycle will generate residual stresses and influence the fiber rearrangement and capillary flow within the fibre tows. For the semi-crystalline PP matrix, a higher cooling rate yields higher residual stresses. The magnitude of the stresses varies depending on several parameters such as number of plies, fibre volume fraction, and processing conditions. To limit the residual stresses, two-rate cooling profile was applied. As shown in Figure 4, the temperature of the composite was reduced to 130°C at the cooling rate of −2.5°C/min by air and subsequently the cooling rate was increased to −10.5°C/min by water to reduce the temperature of the composite to 50°C.

2.3 Sample preparation

Two series of consolidation tests were performed on the Flax/PP prepreg. The first series of experiments were planned for the

assessment of porosity fractions and morphology evolutions by consolidation of 17 Flax/PP prepreg layers. Consolidation was divided into five stages, which contributed to the change in the laminate thickness under the same applied pressure P. Depending on the consolidation's stages, the thickness was reduced from 5.8 mm to 4.5 mm. The second series of experiments were planned for the determination of the in-plane and through-thickness thermal conductivities of Flax/PP composites. To make free-edge effect consolidation, each layer was first punched to the final part dimension. During the consolidation stages, a confined compression mould with a gap of 0.05 mm between upper and bottom mould was used, enabling the air/gas removal without squeezing out the fibres from the mould cavity. Finally, to avoid potential surface effects at the edge area, all samples were cut 10 mm far from the edges.

The thickness of composite samples should be at least 10 mm for thermal conductivity measurements (EN ISO 22007-2:2015, 2015). The samples for thermal conductivity measurements were
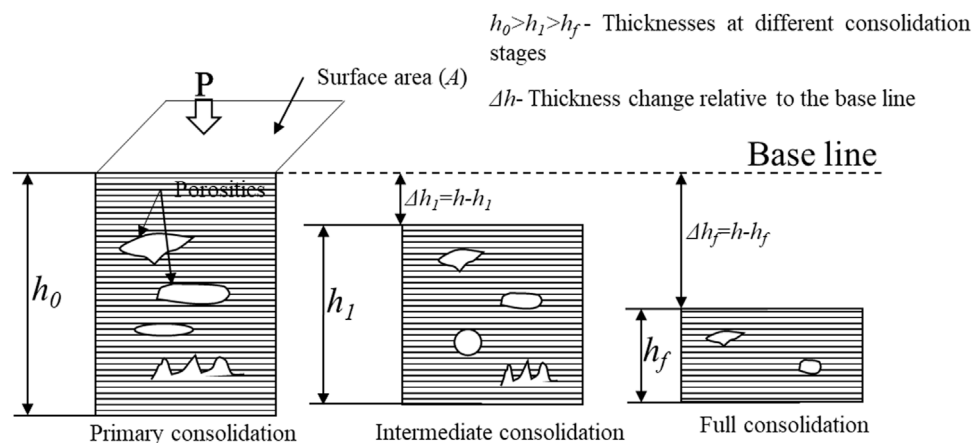
FIGURE 9
the changes in porosity fraction and thicknesses at different stages of consolidation. h_f is the final thickness after the full consolidation.

TABLE 4 Porosity volume fractions relative to the corresponding consolidation stages.

Consolidation stage [laminate thickness (mm)]	Volume of sample (mm³)	Volume of a porosity (µm³)		Volume of total porosity (mm³)	Porosity volume fraction (%)
		Min	Max		
Primary consolidation (5.80)	555.12	8.480×10^{-6}	99.562	107.51	19.36
2 (5.40)	554.44	6.86×10^{-6}	101.918	112.33	20.26
3 (5.00)	569.54	6.86×10^{-6}	19.91	53.76	9.44
4 (4.60)	555.27	8.48×10^{-6}	0.964	14.08	2.53
Full consolidation (4.3)	584.50	8.48×10^{-6}	0.0075	0.085	0.01

approximately three times thicker than those samples used for the measurements of porosity fractions and morphology evolution. Depending on the consolidation's stages, the thicknesses of samples for thermal conductivity measurements were reduced from 16 mm to 12 mm by consolidation of 60 Flax/PP prepreg layers. Table 3 shows series of experiments planned for the fabrication of composites consolidated at different thicknesses.

2.4 Testing

2.4.1 Porosity fraction and morphology evolution
2.4.1.1 Porosity fraction

An Image-based technique, which is a common tool for the assessment of the void content of composites (Machado et al., 2022), was used to assess the porosity fraction. Due to high porosity content, especially for the primary consolidation case, X-ray micro-computed tomography (µ-CT) was employed to obtain three-dimensional (3D) images of porosities inside the consolidated samples. The porosity fraction was estimated from segmented 3D images. As the focus of the current study was to address the relationship of porosity fraction and thermal conductivity, the authors will not discuss the detailed porosity

characteristics such as shape, location, and spatial distribution. The individual samples (10 mm × 10 mm) were scanned on a EasyTOM high-end CT system from RX Solutions with the following operating conditions: voltage: 50 kV; current: 200 µA, isotropic voxel size: 20 × 20 × 20 µm, scan time: 90 min 2,100 radiographic projections were acquired with the rotation step of 0.12° with the exposure time of one second for each projection. The voxel size means that only porosities equal to or larger than equivalent diameters, which is the ratio of the surface area of a pore to its perimeter, of 20 µm were accounted. The reconstruction of the X-ray projections to tomographic slices was performed with RX act software from RX solutions (RX Solutions, 2022). The segmentation and data processing were conducted using the 2D/3D image analysis software Avizo. Another Avizo software feature is the ability to calculate the porosity and analyze the pore connectivity (Li et al., 2021). The porosity fraction of flax/PP at different consolidation stages was then estimated by Avizo. The interactive thresholding module of the Avizo software was applied to return a binary image (porosities in black and flax/pp in gray) (Figure 5A). In the interactive thresholding, the classification of the pore phase and the solid phase (Flax/PP) was performed automatically based on shape characteristics of the image histogram. The module smoothed the histogram to two

FIGURE 10
μ-CT images of samples at different consolidation stages.

FIGURE 11
The longitudinal view of a flax/pp fibre tow.
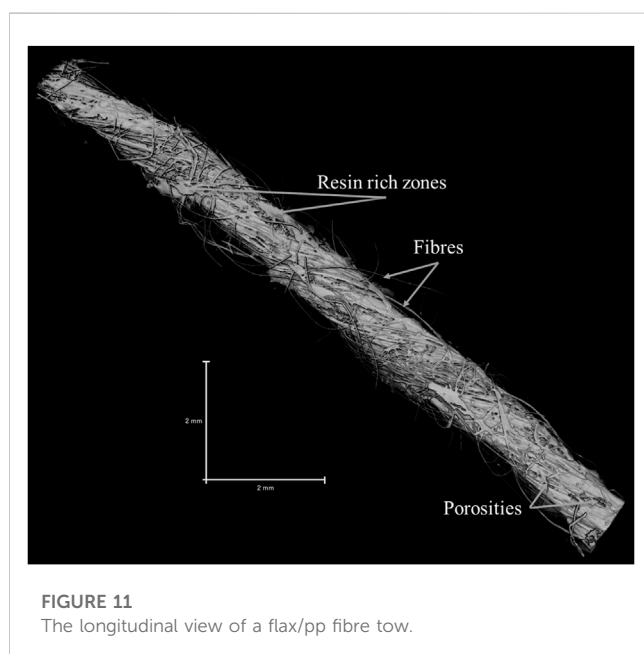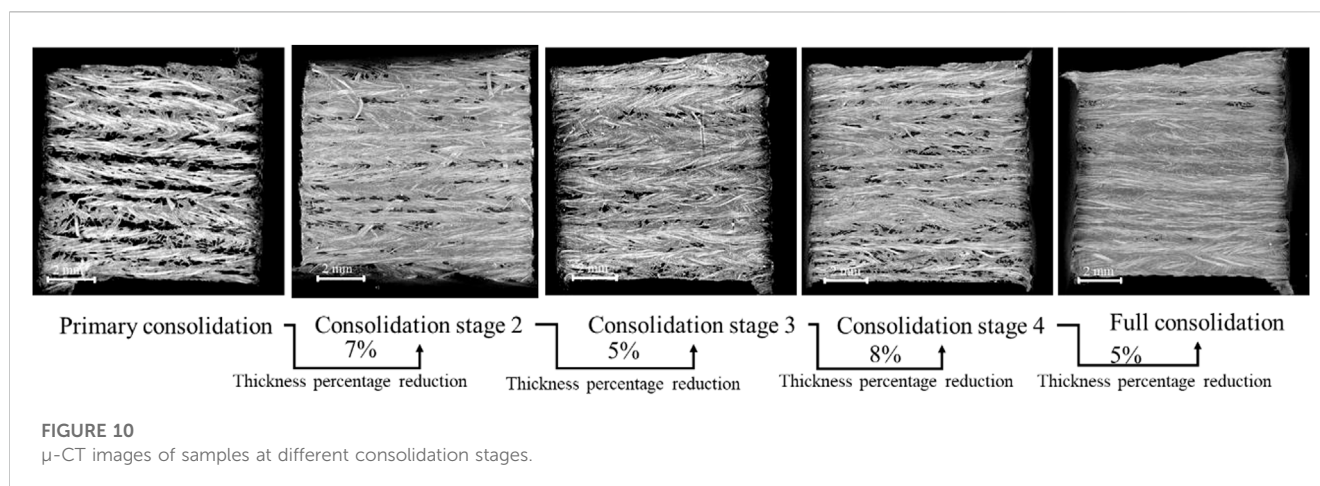
distinguishable peaks, and the valley between these peaks was selected as the threshold value. As the acquired images showed a roughly bimodal histogram, they are appropriated to the interactive thresholding (Sankur, 2004; Jensen et al., 2014). Subsequently a color threshold was imposed to highlight the porosity regions for the estimation of porosity fraction (Figure 5B).

2.4.1.2 Morphology evolution

The cross-sectional morphology evolution of consolidated samples was examined by a pressure-controlled FEI Quanta FEG 200 scanning electron microscope (SEM) from FEI Company (Oregon, United States). For the investigation of morphology evolution, the samples were embedded in low viscosity resin and subsequently were polished to obtain scratch-free surface finishes. The samples with a size of $12 \times 15 \times 15$ mm were cleaned and dried at 80°C for 1 hour and immediately were transferred to the SEM chamber to minimize the moisture absorption of the composites.

Figure 6 shows cross-sectional (6a) and 3D view (6b and c) of a fully consolidated ten-layer Flax/PP composites. The cross-sectional view from Figure 6A reveals the homogeneous distribution of fiber inside the polymer matrix. A fiber volume fraction of 34% and a porosity fraction of 0.7% through the segmented 3D image were estimated by applying Avizo software, confirming the well-consolidated reference sample.

2.4.2 Thermal conductivity measurement

The measurements of thermal conductivity of all composites were conducted at the room temperature and normal pressure by using Hot disk technique [i.e., transient plane source (TPS)]. The sample size used for the measurements was 15×15 mm^2 (Figure 7A). The Hot Disk is a TPS 2500 S from Hot Disk instruments with a Kapton-insulated sensor in the form of a bifilar spiral with the design number of 7,577 (a = 2.001 mm radius) (Figure 7B). Both in-plane and transverse thermal conductivities were measured according to EN ISO 22007–2: 2015. Assuming the conductive pattern to be in the y-z plane of a coordinate system, the in-plane and transverse thermal conductivities were measured, correspondingly (Figure 7B).

For each consolidation stage (Table 3, five configurations), six samples were cut using water jet to produce thermal conductivity test samples (Figure 5A). The Kapton sensor was sandwiched between two samples (Figure 5B). The thermal conductivity of testing samples was determined by monitoring temperature increase of sensor for 10 s due to an input power per unit area, which was increased from 20 to 50 mW with the 10 mW steps. These measurements were repeated three times for each consolidation stage.

3 Results and discussion

3.1 Porosity fraction and morphology evolution

The SEM images of morphology evolution from primary consolidation to full consolidation are shown in Figure 8. Based on the consolidation results on Flax/PP specimens of different
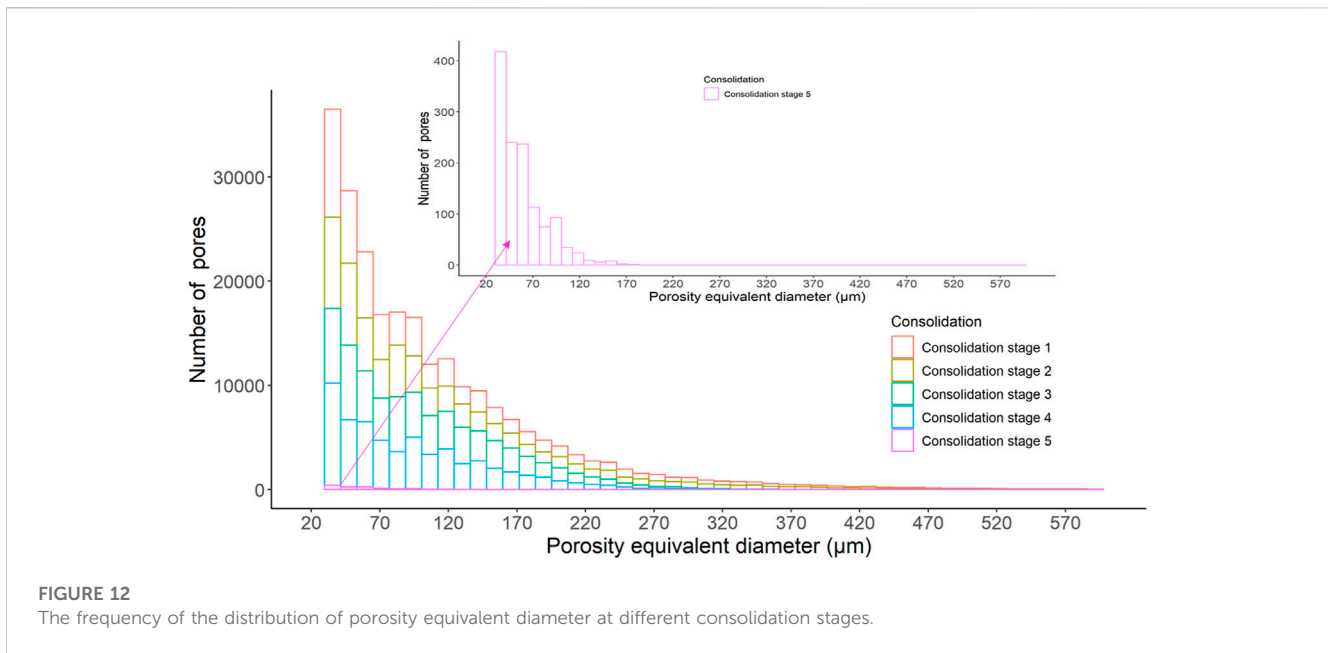
FIGURE 12
The frequency of the distribution of porosity equivalent diameter at different consolidation stages.

TABLE 5 Comparison of the thermal conductivity values obtained for the neat PP. It should be noted that the type of PPs in terms of its amorphous or semicrystalline structure was not addressed by the Refs.

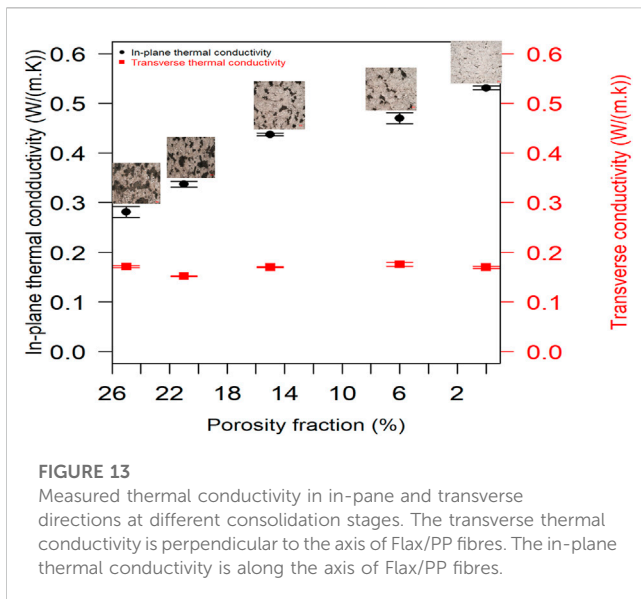| Refs	Supplier	Average thermal conductivity at 25°C (W/(m.k))
Current study (semi-crystalline)		0.16
Muratov et al., (2021) (semi-crystalline)	PP, Borealis	0.18
Krause et al. (2019)	PP, Moplen HP400R	0.26
Chen et al. (2017)	PP, MoplenRP344RK	0.22
Krause and Pötschke (2016)	PP, 579S (sabic)	0.26
Han and Fina (2011)	Not specified	0.11
Weidenfeller et al. (2004)	Minelco B.V. &RTP s.a.r.l	0.22

thickness, when the compression load was applied to the specimens, a decrease in volume is due to the fiber rearrangement (Figure 6 in white color) and a reduction of porosity fraction (Figure 8 in black color). According to Terzaghi (Terzaghi, 1943), a change in volume directly affects the porosity fraction of a saturated porous medium (i.e., flax/PP prepreg), which is evident from Figure 8.

Considering the Terzaghi's one-dimensional consolidation theory, and assuming incompressible fluid, a correlation between the volume of porosity fraction and thickness changes can be explained schematically by Figure 9. Due to the applied pressure (p), the prepreg layers experienced the stress and the porous regions filled by the resin at higher thickness reduction reducing the volume of specimens at different consolidation stages (Nixon-Pearson et al., 2017). This effect is negligible for full consolidation specimen since the void content was below 0.7% from X-ray CT scans.

Therefore, decreasing the thickness from 5.8 mm to 4.3 mm results in a large reduction of the porosity volume fraction from 19.36% to 0.01% at constant pressure (Table 4).

The specific micro-mechanism of the porosity reduction at different consolidation stages includes coupled mechanism of stress equilibrium between porosity internal pressure and porosity compression by applied pressure and porosity filling with the resin flow. Surface tension between the porosities and resin works together with porosity internal pressure and the applied pressure, governing stress equilibrium and whether the porosities should collapse or grow. At the fibre tow scale, as the temperature during the hot press forming was constant, the contribution of resin viscosity which affects the rate of resin flow and critical time for the porosity reduction was not addressed in the current study.

Figure 10 shows extensive inter and intra-layer porosities for the primary consolidation. In the hot press forming process, air entrapment, dissolved and adsorbed moisture and volatiles such as plasticizer in the PP may cause the nucleation and growth of porosities during the forming processing (Figure 10). Consolidation at lower thicknesses tend to show both reduced porosity size and reduced amount of low fiber density areas. A complaint network of

FIGURE 13
Measured thermal conductivity in in-pane and transverse directions at different consolidation stages. The transverse thermal conductivity is perpendicular to the axis of Flax/PP fibres. The in-plane thermal conductivity is along the axis of Flax/PP fibres.

FIGURE 14
Comparison of measured values of the thermal conductivity of Flax/PP laminates in in-plane and transverse direction with two-level Mori-Tanaka model *versus* porosity fraction.

fiber and viscous matrix exhibits various flow and deformation mechanisms depending on applied conditions. Moreover, inadequate resin impregnation into the fibre tows can cause additional porosities. For porosities inside the fiber tow regions, after applying the pressure, the laminate thickness is reduced, and the resin flows through the fibre tows to fill the porosities due to squeezing flow from resin rich zones to fill porous regions (Wang and Gutowski, 1991; Shuler and Advani, 1996; Simacek et al., 2013).

Porosities in Flax/PP composites can be due to the initial porosities in the Flax/PP commingled layers or can be caused due to the air entrapment between layers during laminations. The porosities can vary in size from 20 to 50 microns in the zones of poor impregnation The initial porosities in the prepreg are generated during the manufacturing of the pre-consolidated unidirectional Flax/Polypropylene (PP) commingled tape (Figure 11).

Previous studies revealed that individual porosity characteristics, i.e., porosity content, diameter and aspect ratio are statically distributed in a volume of the consolidated thermoplastic laminate. Figure 12 shows the distribution of the void equivalent diameter at each consolidation stage. As an overall trend, the number of voids sharply skewed right as the porosity equivalent diameter increases, indicating a high small porosity content in the range of 20–100 μm at the each of the consolidation stages. As the consolidation extended from stage 1–5, the maximum number of pores reduced 98%. The authors plan to publish the detailed determination of the statistics of porosity characteristics in Flax/PP laminate.

3.2 Thermal conductivity

3.2.1 Thermal conductivity of PP

The reported thermal conductivity values for the pure consolidated polypropylene (Table 5) can range between 0.1 and 0.3 W/(m.K) at 25°C. Because the thermal conductivity of a polymer, particularly consolidated PP, is a complex function of temperature,
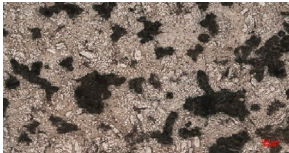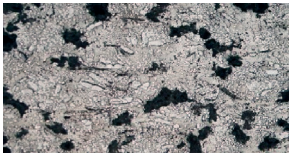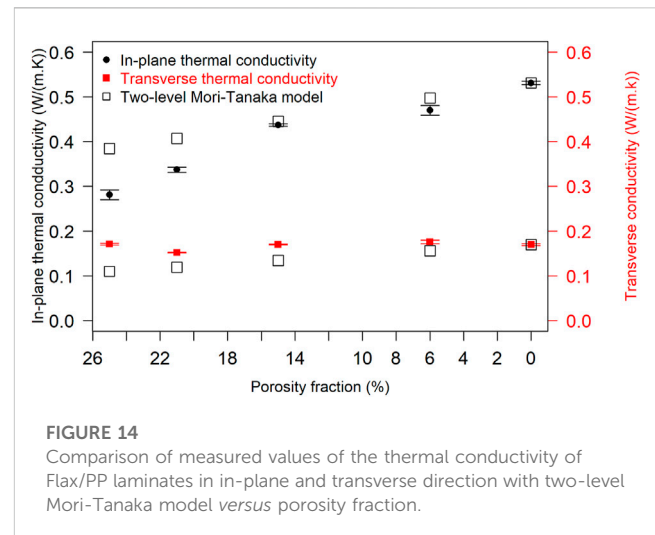
pressure, molecular weight distribution and chain structure (Patti and Acierno, 2020). For the current study, both in-plane and transverse thermal conductivity of the neat PP polymer plate were measured around 0.16 W/(m.k), which is well within the reported range. As the thermal conductivity has the same value in the principal directions, the neat PP was regarded as a homogeneous material.

3.2.2 Thermal conductivity of Flax/PP

The measured thermal conductivities of unidirectional Flax/PP composites in in-plane and transverse directions are plotted as a function of porosity fraction in Figure 13. As the porosity fraction decreases, the in-plane thermal conductivity increases. An increase of 70% occurs from in-plane conductivity equal to 0.28 [W/(m.K)] for the porosity fraction of 25% to 0.53 [W/(m.K)] for the porosity fraction of almost 0%. A decrease in porosity leads to a rise in the number of contact points as well as an increase in the volume of flax/PP fraction (with reference to Figures 6, 8) with much higher thermal conductivity than the thermal conductivity of the air gaps (inter and intra layer porosities) [0.026 W/(m.K)] (Liu et al., 2012) in the whole volume. From Figure 13, it is indicated that the in-plane thermal conductivity is dependent on the degree of Flax/PP fibre packing. At full consolidation stage containing approximately 0% porosity (Figures 10, 13), Flax/PP fibres are very densely packed and touch each other, leading to the highest thermal conductivity (Barasinski et al., 2011; Lévy et al., 2014). As stated in the literature, the transfer of heat in non-metals such as polymer composites can be explained by the flow of phonons or propagation of lattice vibrational energy (Slack, 1979; Ishida and Rimdusit, 1998). Consequently, the maximum packing of the flax fibre in the matrix is one way to maximise the formation of highly thermal conductive networks. Unlike in-plane conductivity, as the porosity fraction decreases the transverse thermal conductivity remains almost constant with an average thermal conductivity of 0.167 W/(k.m). Since Flax/PP commingled fibres consist of flax fibres that are radially arranged around the axis of PP fibres, the thermal path tends to be formed axially rather than transversely cross it. Moreover, as it is also obvious from Figure 13, the in-plane thermal conductivity values are much higher than the transverse

TABLE 6 Morphology evolution and thermal conductivity at different the consolidation stages of flax/PP. As there is no change in transverse thermal conductivity, the results are not presented.

Consolidation stage (%)	Morphology evolution	Porosity fraction (%)	Fiber volume fraction (%)	In-plane thermal conductivity (W/(m.K))	
				Experiment	Model
Primary consolidation		25	25	0.28	0.38
7		21	27	0.33	0.40
12		15	29	0.43	0.44
20		6	32	0.47	0.49
25		0	34	0.53	0.53

ones at the corresponding porosity fractions of Flax/PP laminates. Because thermal conductivity of pure flax fibres along their axis is 1.232 W/(k.m) while transversely to their main axis is 0.17 W/(k.m). These results are consistence with the thermal conductivity measurements for hemp (Behzad and Sain, 2007), flax (Li et al., 2008), bamboo (Takagi et al., 2007), and banana (Annie Paul et al., 2008) embedded into thermoplastic polymers. Therefore, since thermal resistance along the axis of Flax/PP fibre is less than the thermal resistance across the axis, the most portion of heat is transferred along the Flax/PP axis.

3.3 Model analysis of thermal conductivity

The two-level homogenization method proposed in (Naili et al., 2022) for elastic composites and extended to thermal and electrical conductivity in (Koutsawa et al., 2022) is used here to predict the effective thermal conductivity of the three-phase (flax fibers, pores, and polypropylene matrix) NFRC. The two-level method is based on nested homogenization levels. At the deepest level, the real matrix material is homogenized with a first family of reinforcements. The effective material thus obtained plays the role of a fictitious matrix which is reinforced with another set of reinforcements to constitute an upper-level composite. This procedure is repeated until all reinforcements families have been taken in account. In this study, the Mori–Tanaka model (Mori and Tanaka, 1973) is used at a given level to homogenize the basic two-phase composite. The derivation of Mori-Tanaka's model is based on an approximate use of Eshelby's solution (Eshelby, 1957). It is assumed that each inclusion in the real representative volume element (RVE) behaves as if it were isolated in the real matrix. The body is infinite and subjected to the average matrix strains in the real RVE as the far field (remote) strain. The Mori-Tanaka model is very successful in predicting the effective properties of two-phase

composites. In theory, it is restricted to moderate volume fractions of inclusions (less than 25%) but in practice it can give good predictions well beyond this range. The two-level method can deliver excellent predictions when the right choice of the nested homogenization levels is made. It is shown that for reinforcements with different material properties, when going from the deepest level to the upper level, the inclusions should be added from the most compliant to the most rigid. More details on the model's equations can be found in (Koutsawa et al., 2022).

Reverse calculation based on the reference material is used to determine the model input parameters for the flax fibre. Thus, a flax fibre in-plane thermal conductivity of 1.232 W/(m.K) and a transverse thermal conductivity of 0.170 W/(m.K) were determined and used in the theoretical model. The theoretical values present a good agreement with experiments (Figure 14) for low and moderate porosity fractions ($\leq 15\%$). The gap between the model and the experimental data for high porosity fractions ($> 15\%$) can be explained by the simplifying assumptions used in the model regarding the pores' size, aspect ratio and spatial distribution. Indeed, for this first attempt, the pores are assumed to be spherical and randomly distributed in the microstructure. Therefore, extended experimental data will be required for a better description of the microstructure in the theoretical predictive model.

4 Conclusion

In this study, the link between the porosity fraction, morphology evolution and the thermal conductivity of flax fiber reinforced polypropylene composite was investigated. A hot plate forming process experiment allowed to manufacture several plates with different porosity contents depending on the consolidation stages. Subsequently, hot disk technique was applied to measure the thermal conductivity in in-plane and transverse directions. SEM and as micro-CT were used to analysis the cross sections of the laminates in terms of morphology and porosity fractions. Finally, a theoretical model, based on a two-level Mori-Tanaka homogenization method is proposed.

The results of the study as summarized in Table 6 suggested that.

(1) Transverse thermal conductivity was much lower than in-plane thermal conductivity. This means that the most portion of heat is transferred axially along the Flax/PP fibre where each fibre is surrounded with the PP rather than transversely across it.
(2) In-plane thermal conductivity almost linearly increased with the reduction of porosity fraction. However, the transverse thermal conductivity remained constant. The flax fibre compaction into the matrix is one way to increase the Flax/PP interfaces, improving thermal conductive networks.
(3) Considering the three-phases material (porosity, fiber, and polymer matrix), the model results were in a good agreement with experiments, but limited predictivity for porosity fraction above 15%. The aspect ratio for this range of consolidation cannot be considered as spherical and the typical channel shape of porosity must be integrated in the theoretical model.
(4) The morphology evolution should be included in the thermal simulation of composite laminate forming process. The future study aims at developing a simulation tool for the coupling of the microstructure evolution and heat transfer in the hot press forming technique.

We will also address the effects of moisture content on the thermal conductivity of the fully consolidated Flax/PP composite in the future work.

Data availability statement

The raw data supporting the conclusion of this article will be made available by the authors, without undue reservation.

Author contributions

MB: Validation, Methodology, Formal analysis, Visualization, Investigation, Writing-original Draft, Review and Editing, DD: Data Curation, Formal analysis, Review and Editing, N-LS: Methodology, Investigation, ML: Methodology, Investigation, YK: Software, Numerical analysis, Review and Editing. BU: Material supply, material characterisation, HP: Conceptualization, Methodology, Supervision, Validation, Formal analysis, funding acquisition, Visualization, Investigation, Review and Editing.

Funding

Acknowledgments

Conflict of interest

Author BU was employed by BPREG.

The remaining authors declare that the research was conducted in the absence of any commercial or financial relationships that could be construed as a potential conflict of interest.

Publisher's note

All claims expressed in this article are solely those of the authors and do not necessarily represent those of their affiliated

organizations, or those of the publisher, the editors and the reviewers. Any product that may be evaluated in this article, or

claim that may be made by its manufacturer, is not guaranteed or endorsed by the publisher.

References

Ageorges, C., Ye, L., and Hou, M. (2001). Advances in fusion bonding techniques for joining thermoplastic matrix composites: A review. *Compos Part A Appl. Sci. Manuf.* 32, 839–857. doi:10.1016/s1359-835x(00)00166-4

Ageorges, C., and Ye, L. (2002). "State of the art in fusion bonding of polymer composites," in *Fusion bonding of polymer composites* (London: Springer), 7–64. doi:10.1007/978-1-4471-0171-0_2

Annie Paul, S., Boudenne, A., Ibos, L., Candau, Y., Joseph, K., and Thomas, S. (2008). Effect of fiber loading and chemical treatments on thermophysical properties of banana fiber/polypropylene commingled composite materials. *Compos Part A Appl. Sci. Manuf.* 39 (9), 1582–1588. doi:10.1016/j.compositesa.2008.06.004

Barasinski, A., Leygue, A., Soccard, E., and Poitou, A. (2011). *In situ* consolidation for thermoplastic tape placement process is not obvious. *AIP Conf. Proc.* 1353, 948–953. doi:10.1063/1.3589638

Behzad, T., and Sain, M. (2007). Measurement and prediction of thermal conductivity for hemp fiber reinforced composites. *Polym. Eng. Sci.* 47 (7), 977–983. doi:10.1002/pen.20632

Bourmaud, A., le Duigou, A., Gourier, C., and Baley, C. (2016). Influence of processing temperature on mechanical performance of unidirectional polyamide 11-flax fibre composites. *Ind. Crops Prod.* 84, 151–165. doi:10.1016/j.indcrop.2016.02.007

BPREG (2022). Technical sheet. Available at: www.bpreg.com.

Chen, L., Xu, H. F., He, S. J., Du, Y. H., Yu, N. J., Du, X. Z., et al. (2017). Thermal conductivity performance of polypropylene composites filled with polydopamine-functionalized hexagonal boron nitride. *PLoS One* 12 (1), e0170523. doi:10.1371/journal.pone.0170523

Derbali, I., Terekhina, S., Guillaumat, L., and Ouagne, P. (2018). Rapid manufacturing of woven comingled flax/polypropylene composite structures. *Int. J. Material Form.* 12 (6), 927–942. doi:10.1007/s12289-018-01464-1

Donough, M. J., ShafaqSt John, N. A., Philips, A. W., and Gangadhara Prusty, B. (2022). Process modelling of *in-situ* consolidated thermoplastic composite by automated fibre placement – a review. *Compos. Part A Appl. Sci. Manuf.* 163, 107179. doi:10.1016/j.compositesa.2022.107179

Dumont, P. J. J., Orgéas, L., Hubert, M., Vermeulen, B., Vroman, P., Rolland du Roscoat, S., et al. (2010). "Compression moulding of flax fibre reinforced composite materials," in The 10th International Conference on Flow Processes in Composite Materials (FPCM10), Monte Verità, Ascona, CH, July 11-15, 2010.

Dumont, P., Orgéas, L., Martoia, F., Budtova, T., and Vincent, M. (2017). "Mise en œuvre des composites à fibres lignocellulosiques," in *Composites polymères et fibres lignocellulosiques Propriétés, transformation et caractérisation*, Vol. 5, 159–211.

EN ISO 22007-2:2015 (2015). *Plastics-Determination of thermal conductivity and thermal diffusivity.*

Eshelby, J. D. (1957). The determination of the elastic field of an ellipsoidal inclusion, and related problems. *Proc. R. Soc. Lond A Math. Phys. Sci.* 241 (1226), 376–396. doi:10.1098/rspa.1957.0133

Fu, S. Y., and Mai, Y. W. (2003). Thermal conductivity of misaligned short-fiber-reinforced polymer composites. *J. Appl. Polym. Sci.* 88 (6), 1497–1505. doi:10.1002/app.11864

Fu, X., Wu, X., Huang, G., Li, W., Kang, S., Wang, L., et al. (2022). Fusion bonding possibility for incompatible polymers by the novel ultrasonic welding technology: Effect of interfacial compatibilization. *ACS Omega* 7 (17), 14797–14806. doi:10.1021/acsomega.2c00255

Fujihara, K., Huang, Z.-M., Ramakrishna, S., and Hamada, H. (2004). Influence of processing conditions on bending property of continuous carbon fiber reinforced PEEK composites. *Compos. Sci. Technol.* 64 (16), 2525–2534. doi:10.1016/j.compscitech.2004.05.014

Gassan, J., and Bledzki, A. K. (2001). Thermal degradation of flax and jute fibers. *J. Appl. Polym. Sci.* 82 (6), 1417–1422. doi:10.1002/app.1979

Guzman-Maldonado, E., Hamila, N., Naouar, N., Moulin, G., and Boisse, P. (2016). Simulation of thermoplastic prepreg thermoforming based on a visco-hyperelastic model and a thermal homogenization. *Mater Des.* 93, 431–442. doi:10.1016/j.matdes.2015.12.166

Han, S., and Chung, D. D. L. (2011). Increasing the through-thickness thermal conductivity of carbon fiber polymer–matrix composite by curing pressure increase and filler incorporation. *Compos. Sci. Technol.* 71 (16), 1944–1952. doi:10.1016/j.compscitech.2011.09.011

Han, Z., and Fina, A. (2011)., 36. Oxford, 914–944. doi:10.1016/j.progpolymsci.2010.11.004Thermal conductivity of carbon nanotubes and their polymer nanocomposites: A reviewProg. Polym. Sci.7

Hernández, S., Sket, F., González, C., and Llorca, J. (2013). Optimization of curing cycle in carbon fiber-reinforced laminates: Void distribution and mechanical properties. *Compos Sci. Technol.* 85, 73–82. doi:10.1016/j.compscitech.2013.06.005

il Lee, W., and Springer, G. S. (1987). A model of the manufacturing process of thermoplastic matrix composites. *J. Compos Mater* 21 (11), 1017–1055. doi:10.1177/002199838702101103

Ishida, H., and Rimdusit, S. (1998). Very high thermal conductivity obtained by boron nitride-filled polybenzoxazine. *Thermochimica* 320, 177–186. doi:10.1016/s0040-6031(98)00463-8

Jensen, S., Samanta, S., Chakrabarti-Bell, S., Regenauer-Lieb, K., Siddique, K. H. M., and Wang, S. (2014). Automated thresholding and analysis of microCT scanned bread dough. *J. Microsc.* 256 (2), 100–110. doi:10.1111/jmi.12163

Khan, M. A., Mitschang, P., and Schledjewski, R. (2010). Identification of some optimal parameters to achieve higher laminate quality through tape placement process. *Adv. Polym. Technol.* 29 (2), 98–111. doi:10.1002/adv.20177

Kim, S. W., Lee, S. H., Kang, J. S., and Kang, K. H. (2006). Thermal conductivity of thermoplastics reinforced with natural fibers. *Int. J. Thermophys.* 27 (6), 1873–1881. doi:10.1007/s10765-006-0128-0

Koutsawa, Y., Rauchs, G., Fiorelli, D., Makradi, A., and Belouettar, S. (2022). A multi-scale model for the effective electro-mechanical properties of short fiber reinforced additively manufactured ceramic matrix composites containing carbon nanotubes. *Compos. Part C. Open Access* 7, 100234. doi:10.1016/j.jcomc.2022.100234

Krause, B., and Pötschke, P. (2016). Electrical and thermal conductivity of polypropylene filled with combinations of carbon fillers. *AIP Conf. Proc.* 1779. doi:10.1063/1.4965494

Krause, B., Rzeczkowski, P., and Pötschke, P. (2019). Thermal conductivity and electrical resistivity of melt-mixed polypropylene composites containing mixtures of carbon-based fillers. *Polym. (Basel)* 11, 1073–1076. doi:10.3390/POLYM11061073

Lamèthe, J. F., Beauchêne, P., and Léger, L. (2005). Polymer dynamics applied to PEEK matrix composite welding. *Aerosp. Sci. Technol.* 9 (3), 233–240. doi:10.1016/j.ast.2005.01.008

Latil, P., Orgéas, L., Geindreau, C., Dumont, P. J. J., and Rolland du Roscoat, S. (2011). Towards the 3D *in situ* characterisation of deformation micro-mechanisms within a compressed bundle of fibres. *Compos Sci. Technol.* 71 (4), 480–488. doi:10.1016/j.compscitech.2010.12.023

Lévy, A., Heider, D., Tierney, J., Gillespie, J., and Levy, A. (2014). Inter-layer thermal contact resistance evolution with the degree of intimate contact in the processing of thermoplastic composite laminates. *Compos. Mater.* 48 (4), 491–503. doi:10.1177/0021998313476318

Li, X., Tabil, L. G., Oguocha, I. N., and Panigrahi, S. (2008). Thermal diffusivity, thermal conductivity, and specific heat of flax fiber–HDPE biocomposites at processing temperatures. *Compos Sci. Technol.* 68 (7–8), 1753–1758. doi:10.1016/j.compscitech.2008.02.016

Li, Y., Chi, Y., Han, S., Zhao, C., and Miao, Y. (2021). Pore-throat structure characterization of carbon fiber reinforced resin matrix composites: Employing Micro-CT and Avizo technique. *PLoS One* 16 (9), e0257640. doi:10.1371/journal.pone.0257640

Liu, K., Takagi, H., Osugi, R., and Yang, Z. (2012). Effect of physicochemical structure of natural fiber on transverse thermal conductivity of unidirectional abaca/bamboo fiber composites. *Compos Part A Appl. Sci. Manuf.* 43 (8), 1234–1241. doi:10.1016/j.compositesa.2012.02.020

Liu, K., Zhang, X., Takagi, H., Yang, Z., and Wang, D. (2014). Effect of chemical treatments on transverse thermal conductivity of unidirectional abaca fiber/epoxy composite. *Compos Part A Appl. Sci. Manuf.* 66, 227–236. doi:10.1016/j.compositesa.2014.07.018

Lu, J., Kan, A., Zhu, W., and Yuan, Y. (2021). Numerical investigation on effective thermal conductivity of fibrous porous medium under vacuum using Lattice-Boltzmann method. *Int. J. Therm. Sci.* 160, 106682. doi:10.1016/j.ijthermalsci.2020.106682

Lukaszewicz, D. H. J. A., Ward, C., and Potter, K. D. (2012). The engineering aspects of automated prepreg layup: History, present and future. *Compos B Eng.* 43 (3), 997–1009. doi:10.1016/j.compositesb.2011.12.003

Machado, J. M., Tavares, J. M. R. S., Camanho, P. P., and Correia, N. (2022). Automatic void content assessment of composite laminates using a machine-learning approach. *Compos Struct.* 288, 115383. doi:10.1016/j.compstruct.2022.115383

Madsen, B., Thygesen, A., and Lilholt, H. (2007). Plant fibre composites - porosity and volumetric interaction. *Compos. Sci. Technol.* 67 (7–8), 1584–1600. doi:10.1016/j.compscitech.2006.07.009

Mangal, R., Saxena, N. S., Joshi, G. P., and Thomas, S. (2003). Measurement of effective thermal conductivity and thermal diffusivity for assessing the integrity of fiber to matrix bond in natural fiber composite. *Indian J. Pure Appl. Phys.* 41 (9), 712–718.

Mantell, S. C., and Springer, G. S. (1992). Manufacturing process models for thermoplastic composites. *J. Compos Mater* 26 (16), 2348–2377. doi:10.1177/002199839202601602

Mehdikhani, M., Gorbatikh, L., Verpoest, I., and v Lomov, S. (2019). Voids in fiber-reinforced polymer composites: A review on their formation, characteristics, and effects on mechanical performance. *J. Compos Mater* 53 (12), 1579–1669. doi:10.1177/0021998318772152

Mishra, R., Wiener, J., Militky, J., Petru, M., Tomkova, B., and Novotna, J. (2020). Bio-composites reinforced with natural fibers: Comparative analysis of thermal, static and dynamic-mechanical properties. *Fibers Polym.* 21 (3), 619–627. doi:10.1007/s12221-020-9804-0

Mori, T., and Tanaka, K. (1973). Average stress in matrix and average elastic energy of materials with misfitting inclusions. *Acta Metall.* 21 (5), 571–574. doi:10.1016/0001-6160(73)90064-3

Mounika, M., Ramaniah, K., Ratna Prasad, A. V., Rao, K. M., Hema, K., and Reddy, C. (2012). Thermal conductivity characterization of bamboo fiber reinforced polyester composite. *J. Mater. Environ. Sci.* 3 (6), 1109–1116.

Muratov, D. S., Vanyushin, V. O., Luchnikov, L. O., Degtyaryov, M. Y., Kolesnikov, E. A., Stepashkin, A. A., et al. (2021). Improved thermal conductivity of polypropylene filled with exfoliated hexagonal boron nitride (hBN) particles. *Mater Res. Express* 8 (3), 035010. doi:10.1088/2053-1591/abed0f

Naili, C., Doghri, I., and Demey, J. (2022). Porous materials reinforced with short fibers: Unbiased full-field assessment of several homogenization strategies in elasticity. *Mech. Adv. Mater. Struct.* 29 (20), 2857–2872. doi:10.1080/15376494.2021.1880674

Nixon-Pearson, O. J., Belnoue, J. P. H., Ivanov, D. S., Potter, K. D., and Hallett, S. R. (2017). An experimental investigation of the consolidation behaviour of uncured prepregs under processing conditions. *J. Compos Mater* 51 (13), 1911–1924. doi:10.1177/0021998316665681

Ouagne, P., Bizet, L., Baley, C., and Bréard, J. (2010). Analysis of the film-stacking processing parameters for PLLA/flax fiber biocomposites. *J. Compos Mater* 44 (10), 1201–1215. doi:10.1177/0021998309349019

Patti, A., and Acierno, D. (2020). "Thermal conductivity of polypropylene-based materials," in *Polypropylene - polymerization and characterization of mechanical and thermal properties* (London, UK: IntechOpen). doi:10.5772/intechopen.84477

RX Solutions (2022). *RX ACT software*. Chennai, TN: RX solutions.

Saenz-Castillo, D., Martín, M. I., Calvo, S., Rodriguez-Lence, F., and Güemes, A. (2019). Effect of processing parameters and void content on mechanical properties and NDI of thermoplastic composites. *Compos Part A Appl. Sci. Manuf.* 121, 308–320. doi:10.1016/j.compositesa.2019.03.035

Sankur, B. (2004). Survey over image thresholding techniques and quantitative performance evaluation. *J. Electron Imaging* 13 (1), 146. doi:10.1117/1.1631315

Shuler, S. F., and Advani, S. G. (1996). Transverse squeeze flow of concentrated aligned fibers in viscous fluids. *J. Newt. Fluid Mech.* 65, 47. doi:10.1016/0377-0257(96)01440-1

Simacek, P., Advani, S. G., Gruber, M., and Jensen, B. (2013). A non-local void filling model to describe its dynamics during processing thermoplastic composites. *Compos Part A Appl. Sci. Manuf.* 46, 154–165. doi:10.1016/j.compositesa.2012.10.015

Slack, G. A. (1979). The thermal conductivity of nonmetallic crystals. *Solid State Phys.* 34, 1–71. doi:10.1016/S0081-1947(08)60359-8

Takagi, H., Kako, S., Kusano, K., and Ousaka, A. (2007). Thermal conductivity of PLA-bamboo fiber composites. *Adv. Compos. Mater. Official J. Jpn. Soc. Compos. Mater.* 16 (4), 377–384. doi:10.1163/156855107782325186

Terzaghi, K. (1943). *Theoretical soil mechanics*. Hoboken, NJ, USA: John Wiley & Sons. doi:10.1002/9780470172766

Thilagavathi, G., Pradeep, E., Kannaian, T., and Sasikala, L. (2010). Development of natural fiber nonwovens for application as car interiors for noise control. *J. Industrial Text.* 39 (3), 267–278. doi:10.1177/1528083709347124

Tierney, J., and Gillespie, J. W. (2006). Modeling of *in situ* strength development for the thermoplastic composite tow placement process. *J. Compos Mater* 40 (16), 1487–1506. doi:10.1177/0021998306060162

van de Velde, K., and Baetens, E. (2001). Thermal and mechanical properties of flax fibres as potential composite reinforcement. *Macromol. Mater Eng.* 286 (6), 342–349. doi:10.1002/1439-2054(20010601)286:6<342::AID-MAME342>3.0.CO;2-P

van Hoa, S., Duc Hoang, M., and Simpson, J. (2017). Manufacturing procedure to make flat thermoplastic composite laminates by automated fibre placement and their mechanical properties. *J. Thermoplast. Compos. Mater.* 30 (12), 1693–1712. doi:10.1177/0892705716662516

van Rijswijk, K., and Bersee, H. E. N. (2007). Reactive processing of textile fiber-reinforced thermoplastic composites - an overview. *Compos. Part A Appl. Sci. Manuf.* 38 (3), 666–681. doi:10.1016/j.compositesa.2006.05.007

Wang, C., Zuo, Q., Lin, T., Anuar, N. I. S., Mohd Salleh, K., Gan, S., et al. (2020). Predicting thermal conductivity and mechanical property of bamboo fibers/polypropylene nonwovens reinforced composites based on regression analysis. *Int. Commun. Heat Mass Transf.* 118, 104895. doi:10.1016/j.icheatmasstransfer.2020.104895

Wang, E. L., and Gutowski, T. G. (1991). Laps and gaps in thermoplastic composites processing. *Compos. Manuf.* 2, 69–78. doi:10.1016/0956-7143(91)90182-G

Weidenfeller, B., Höfer, M., and Schilling, F. R. (2004). Thermal conductivity, thermal diffusivity, and specific heat capacity of particle filled polypropylene. *Compos Part A Appl. Sci. Manuf.* 35 (4), 423–429. doi:10.1016/j.compositesa.2003.11.005

Yang, F., and Pitchumani, R. (2001). A fractal Cantor set based description of interlaminar contact evolution during thermoplastic composites processing. *J. Mater Sci.* 36 (19), 4661–4671. doi:10.1023/A:1017950215945

Yousefpour, A., Hojjati, M., and Immarigeon, J. P. (2004). Fusion bonding/welding of thermoplastic composites. *J. Thermoplast. Compos. Mater.* 17 (4), 303–341. doi:10.1177/0892705704045187

Zhang, D., Heider, D., and Gillespie, J. W. (2017). Determination of void statistics and statistical representative volume elements in carbon fiber-reinforced thermoplastic prepregs. *J. Thermoplast. Compos. Mater.* 30 (8), 1103–1119. doi:10.1177/0892705715618002

Zheng, G. Y. (2014). Numerical investigation of characteristic of anisotropic thermal conductivity of natural fiber bundle with numbered lumens. *Math. Probl. Eng.* 2014, 1–8. doi:10.1155/2014/506818